International Journal of Machine Tools & Manufacture 50 (2010) 1–8

Contents lists available at ScienceDirect

International Journal of Machine Tools & Manufacture

journal homepage: www.elsevier.com/locate/ijmactool

Process analysis for laser solid forming of thin-wall structure

Hua Tan, Jing Chen, Fengying Zhang, Xin Lin, Weidong Huang *

State Key Laboratory of Solidification Processing, Northwestern Polytechnical University, Xi'an 710072, PR China

ARTICLE INFO

Article history:
Received 20 April 2009
Received in revised form
5 October 2009
Accepted 7 October 2009
Available online 4 November 2009

Keywords:
Laser solid forming
Thermal analysis
Deposition thickness
Process improvement

ABSTRACT

Laser solid forming (LSF) is a promising manufacturing technology. Thermal behavior is very significant for the research of microstructure, performance and geometric dimension of the fabricated part. In this research, a two-dimensional transient analytical model was developed on a moving square heat source with a uniform heat intensity distribution, and applied to estimate the temperature distribution and deposition thickness of the LSF thin-wall structures. The effects of two ends of the thin-wall structure and the temperature decline after closing the laser beam were investigated. The deposition thickness with different process parameters was also calculated and agreed well with the data measured by a CCD camera system under the practical process parameters despite some differences. Finally, a unique strategy (adjusting the dwell time of laser beam at both ends) was proposed to improve the dimensional accuracy at two ends of the thin-wall sample, and the experimental results demonstrated the validity of the strategy proposed.

1. Introduction

Laser solid forming (LSF) is a promising manufacturing technology that can build three-dimensional metallic parts directly from CAD model. During LSF, a laser beam scans on a substrate (or a previous clad layer) to create a moving molten pool into which metallic powders are injected through the powder nozzle synchronously. As powders are caught by the moving molten pool and then experience melting and re-solidification process, a clad layer is formed. Further, a three-dimensional part can be built in layer-by-layer fashion. This technique can significantly reduce the length of time between initial concept and finished part. It also allows the production of graded materials and the repair of damaged parts. Several similar methods have been developed to produce metallic parts, such as laser engineered net shaping (LENS) [1], direct laser fabrication (DLF) [2,3], directed metal deposition (DMD) [4,5], and laser-based additive manufacturing (LBAM) [6].

Understanding thermal behavior in the LSF process is significantly helpful to research the microstructure, performance and geometric dimension of a deposited part. Therefore, many studies have been focused on this field. Griffith et al. [7] used the thermocouple and imaging techniques to monitor the thermal signature during LENS process and discussed the solidification behavior, residual stress, and microstructure evolution with respect to thermal behavior. Doubenskaia et al. [8] applied the pyrometer for surface temperature monitoring to control melting/solidification and avoid thermal decomposition in Nd:YAG laser cladding. Pinkerton and Li [9] developed a simple thermal model to analyze the temperature distribution and estimate the molten pool size in laser cladding. Liu and Li [10] established a model to investigate the effects of process variables on laser direct formation of thin wall. Jendrzejewski et al. [11] developed a two-dimensional thermal model to understand the temperature distribution in laser multi-layer cladding. However, the previous models mostly focused on analyzing the steady-state process, and hardly consider the influences of the transient stage and the edges of the samples.

In this research, a two-dimensional transient model was developed to estimate the LSF thin-wall process by using a moving square heat source with uniform heat intensity. The effects of two ends of the thin-wall structure and the temperature decline after closing the laser beam on the thermal behavior were investigated. The deposition thickness with different process parameters were predicted and compared with the experimental data. Further, the process improvement was also discussed.

2. Process model

2.1. Thermal analysis

Fig. 1 is a schematic of the LSF, a thin-wall sample. A laser beam creates a moving molten pool on the top surface of the deposited thin wall with the travel of the CNC table, and the metallic powders are simultaneously conveyed into the molten pool from the nozzle by carrier gas. A clad layer is formed with the

* Corresponding author. Tel./fax: +86 29 8849 4001.
E-mail address: huang@nwpu.edu.cn (W. Huang).

0890-6955/$ - see front matter © 2009 Elsevier Ltd. All rights reserved.
doi:10.1016/j.ijmachtools.2009.10.003

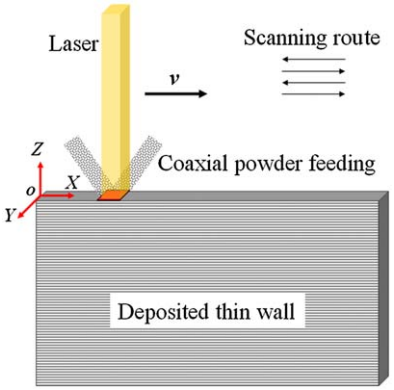

Fig. 1. Schematic of the LSF, a thin-wall sample.

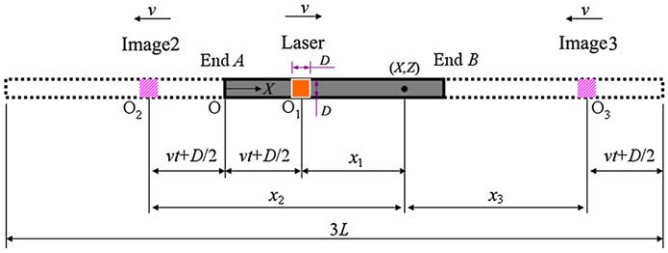

Fig. 2. Schematic of the heat transfer model on the top surface of the thin wall.

solidification of powders caught by the molten pool, and the thin-wall sample is built by multi-layer deposition by following the scanning route (shown in Fig. 1) with an enough interval time between the two layers. In this study, the thickness of the thin wall is much less than the height and length of the wall; so the thermal analysis is considered as a two-dimensional conduction solution in the *X*–*O*–*Z* plane. In addition, our previous research showed that the heat absorbed by powders injected into the molten pool is much less than that absorbed by the substrate [12], so the cooling effect of powders is assumed to be insignificant and is neglected to simplify the analysis.

Fig. 2 is a schematic of the top view of the heat transfer model used for the thin-wall deposition. In this case, the laser spot is considered as a moving square heat source with side length D and with a uniform heat intensity distribution. A thin-wall sample with length L is built as the laser beam scans in a distance of L–D. The thickness of the deposited thin wall is considered as the side length of the laser spot. To investigate the effects of the two ends on the thermal behavior, the method of images [13] is introduced in the analysis. "Image2" and "Image3" are the two image heat sources corresponding to the end A and end B, respectively. O_1, O_2 and O_3 (shown in Fig. 2) are the centers of the actual heat source (laser beam), the image heat source "Image2" and the image heat source "Image3", respectively. OX is the X-axis of the absolute coordinate system, and O_1x, O_2x and O_3x are the x-axis of the three moving coordinate systems corresponding to the actual heat source and the two image heat sources. So any point (X, Z) in the absolute coordinate system can be described as (x_1, z), (x_2, z) and (x_3, z) in the three moving coordinate systems, respectively. In this study, it is assumed that both the laser power and the travel speed of the CNC table reach the set values instantly at the beginning, and decrease to zero instantly at the end of the scanning.

According to Rosenthal's solution for an infinite thin plate [14], the solution of a moving line heat source for a semi-infinite thin wall is expressed as

$$T(x,z,t)=\frac{q}{2\pi\lambda w}\exp\left(-\frac{vx}{2\alpha}\right)\int_0^t\frac{dt'}{t'}\exp\left[-\left(\frac{v^2t'}{4\alpha}+\frac{r^2}{4\alpha t'}\right)\right]+T_0 \quad (1)$$

where $r^2=x^2+z^2$, x, z are the coordinates of the point in the moving coordinate system, q is the heat flow rate of the line heat source, v represents the laser scanning velocity, α denotes the thermal diffusivity, λ is the thermal conductivity, T_0 stands for the initial temperature, t is the time, and w is the thickness of the thin-wall structure. Eq. (1) is used as a basis for the derivations to follow.

A square heat source with a uniform heat intensity distribution can be considered as the equivalent of the combination of a series of moving line heat sources with the length D ($D=w$ in this case), and the heat flow rate q' of the equivalent line heat source can be given by

$$q'=\frac{P\beta}{D}dm \quad (2)$$

where P is the laser power, β is the laser absorptivity, and m is the x-coordinate of any line heat source in moving coordinate system (m varies from $-D/2$ to $D/2$).

Using Eq. (1), the differential temperature at any point (x, z) in the moving coordinate system caused by the equivalent line heat source is given by (considering the origin of the moving coordinate system to coincide with the square heat source center)

$$dT(x,z,t)=\frac{P\beta}{2\pi\lambda wD}\exp\left[-\frac{v(x-m)}{2\alpha}\right]\int_0^t\frac{dt'}{t'}\exp\left\{-\left[\frac{v^2t'}{4\alpha}+\frac{(x-m)^2+z^2}{4\alpha t'}\right]\right\}dm \quad (3)$$

By the integration of Eq. (3), the temperature rise at any point (x, z) in the moving coordinate system and at any time t caused by the entire square heat source is expressed as

$$\Delta T(x,z,t)=\int_{-\frac{D}{2}}^{\frac{D}{2}}\frac{P\beta}{2\pi\lambda wD}\exp\left[-\frac{v(x-m)}{2\alpha}\right]\times\int_0^t\frac{dt'}{t'}\exp\left\{-\left[\frac{v^2t'}{4\alpha}+\frac{(x-m)^2+z^2}{4\alpha t'}\right]\right\}dm \quad (4)$$

From the geometric relationship shown in Fig. 2 and the coordinate transformation, the temperature rise at any point (X, Z) in the absolute coordinate system caused by each of the three heat sources (i.e., the actual moving heat source and its two fictitious image heat sources) is described by

$$\Delta T_1(X,Z,t)=\int_{-\frac{D}{2}}^{\frac{D}{2}}\frac{P\beta}{2\pi\lambda wD}\exp\left\{-\frac{v(x_1-m)}{2\alpha}\right\}\times\int_0^t\frac{dt'}{t'}\exp\left\{-\left[\frac{v^2t'}{4\alpha}+\frac{(x_1-m)^2+z^2}{4\alpha t'}\right]\right\}dm \quad (5)$$

$$\Delta T_2(X,Z,t)=\int_{-\frac{D}{2}}^{\frac{D}{2}}\frac{P\beta}{2\pi\lambda wD}\exp\left[-\frac{v(x_2-m)}{2\alpha}\right]\times\int_0^t\frac{dt'}{t'}\exp\left\{-\left[\frac{v^2t'}{4\alpha}+\frac{(x_2-m)^2+z^2}{4\alpha t'}\right]\right\}dm \quad (6)$$

$$\Delta T_3(X,Z,t)=\int_{-\frac{D}{2}}^{\frac{D}{2}}\frac{P\beta}{2\pi\lambda wD}\exp\left[-\frac{v(x_3-m)}{2\alpha}\right]\times\int_0^t\frac{dt'}{t'}\exp\left\{-\left[\frac{v^2t'}{4\alpha}+\frac{(x_3-m)^2+z^2}{4\alpha t'}\right]\right\}dm \quad (7)$$